

Production of Electron Neutrinos at Nuclear Power Reactors and the Prospects for Neutrino Physics

B. Xin,^{1,2} H.T. Wong,^{2,*} C.Y. Chang,^{2,3} C.P. Chen,² H.B. Li,² J. Li,^{4,5} F.S. Lee,²
S.T. Lin,² V. Singh,² F. Vannucci,⁶ S.C. Wu,² Q. Yue,^{4,5} and Z.Y. Zhou¹

(TEXONO Collaboration)

¹ *Department of Nuclear Physics, Institute of Atomic Energy, Beijing 102413, China.*

² *Institute of Physics, Academia Sinica, Taipei 115, Taiwan.*

³ *Department of Physics, University of Maryland, College Park MD 20742, U.S.A.*

⁴ *Institute of High Energy Physics, Chinese Academy of Science, Beijing 100039, China.*

⁵ *Department of Engineering Physics, Tsing Hua University, Beijing 100084, China.*

⁶ *LPNHE, Université de Paris VII, Paris 75252, France*

(Dated: December 2, 2024)

High flux of electron neutrinos(ν_e) is produced at nuclear power reactors through the decays of nuclei activated by neutron capture. Realistic simulation studies on the neutron transport and capture at the reactor core were performed. The production of ^{51}Cr and ^{55}Fe give rise to mono-energetic ν_e 's at Q-values of 753 keV and 231 keV and fluxes of 8.3×10^{-4} and 3.0×10^{-4} ν_e /fission, respectively. Using data from a germanium detector at the Kuo-Sheng Power Plant, direct limits on the ν_e magnetic moment and the radiative lifetime of $\mu_\nu(\nu_e) < 1.3 \times 10^{-8} \mu_B$ and $\tau_\nu/m_\nu > 0.04 \text{ s} \cdot \text{eV}^{-1}$ at 90% confidence level, respectively, were derived. The ν_e flux can be enhanced by loading selected isotopes to the reactor core, and the potential applications and achievable sensitivities were examined. These include accurate cross-section measurements, searches of the θ_{13} mixing angle and the monitoring of plutonium production.

PACS numbers: 14.60.Lm, 13.15.+g, 28.41.-i

Results from recent neutrino experiments provide strong evidence for neutrino oscillations due to finite neutrino masses and mixings[1, 2]. Their physical origin and experimental consequences are not fully understood. Studies on the neutrino properties and interactions can shed light on these fundamental questions and constrain theoretical models necessary for the interpretation of future precision data. It is motivated to explore alternative neutrino sources. The theme of this paper is to study the production of electron neutrinos(ν_e) from the nuclear power reactors, and their *achievable* physics potentials in ideal experiments.

Production of electron anti-neutrinos($\bar{\nu}_e$) due to β -decays of fission products at the power reactors is a well-studied process[3]. The typical fission rate at the reactor core with a thermal power of P_{th} in GW is $0.3 \times 10^{20} P_{\text{th}} \text{ s}^{-1}$, while an average about 6 $\bar{\nu}_e$ /fission are emitted. The modeling of the $\bar{\nu}_e$ energy spectra above 3 MeV is consistent with measurements at the $<5\%$ level[4], while the low energy portion is subjected to much bigger uncertainties[3]. In a realistically achievable setting for a location 10 m from a core with $P_{\text{th}}=4.5$ GW, the $\bar{\nu}_e$ flux is $6.4 \times 10^{13} \text{ cm}^{-2}\text{s}^{-1}$.

Nuclear reactors also produce ν_e via (a) electron capture or inverse beta decay of fission products and (b) neutron activation on the fuel rods and the construction materials at the reactor core. There were unpublished studies[5] on the reactor ν_e fluxes from the early reactor experiments, indicating that they would not be background to the measurements with $\bar{\nu}_e$. We extended these

studies with realistic simulations focused on the potentials of using them as sources to study neutrino physics.

Primary fission daughters are pre-dominantly neutron-rich and go through β^- -decays to reach stability. Direct feeding to isotopes which decay by β^+ -emissions or electron capture(EC) is extremely weak, at the $\sim 10^{-8}$ /fission level[6]. The leading components for the ^{235}U and ^{239}Pu fissions with relative contributions r_f , fission yields Y_f and branching ratio BR for ν_e -emissions are shown in Table Ia. The average ν_e -yield per fission Y_ν is therefore $Y_\nu = r_f \cdot Y_f \cdot \text{BR}$. In addition, stable fission products can undergo (n, γ) capture to unstable states which decay by ν_e -emissions. The equilibrium yield of the leading components are shown in Table Ib. The leading contribution[6] is from $^{103}\text{Rh}(n, \gamma)^{104}\text{Rh}$ with an average of $\sim 5 \times 10^{-5}$ ν_e /fission emitted during 18 months of irradiation.

A complete ‘‘MCNP’’ neutron transport simulation[7] was performed to study the effect of neutron capture on the reactor core materials, which consists of the fuel elements, cooling water, the control rod structures and the construction materials. The reactor core materials and their mass compositions are summarized in Table II. A homogeneous distribution of these materials inside a stainless steel containment vessel of thickness 22 cm was adopted. This approximation is commonly used and has been demonstrated to be valid in reactor design studies[8]. While the layout is generic for most nuclear power reactors, the exact dimensions and material compositions were derived from the $P_{\text{th}}=2.9$ GW Core#1

TABLE I: The leading ν_e -yields per fission ($Y_\nu = r_f \cdot Y_f \cdot \text{BR}$) from (a) direct feeding of daughters (Z,N) and (b) neutron capture on stable isotope (Z,N-1) at equilibrium condition.

(a)					
Series	(Z,N)	$Y_f(\text{Z,N})$	Q(MeV)	BR(%)	Y_ν
^{235}U ($r_f = 0.5$)	^{86}Rb	$1.4e^{-5}$	0.53	0.005	$3.5e^{-10}$
	^{87}Sr	$<1e^{-5}$	0.2	0.3	$<1.5e^{-8}$
	^{104}Rh	$7e^{-8}$	1.15	0.4	$1.5e^{-10}$
	^{128}I	$1.2e^{-8}$	1.26	6	$3.5e^{-10}$
^{239}Pu ($r_f = 0.35$)	^{128}I	$1.7e^{-6}$	1.26	6	$3.5e^{-8}$
	^{110}Ag	$1.3e^{-5}$	0.88	0.3	$1.4e^{-8}$

(b)						
Series	(Z,N-1)	$Y_f(\text{A-1})$	$\sigma_{n\gamma}(\text{b})$	Q(MeV)	BR(%)	Y_ν
^{235}U ($r_f = 0.5$)	^{104}Rh	$3.2e^{-2}$	146	1.15	0.4	$6.5e^{-5}$
	^{128}I	$1.2e^{-3}$	6.2	1.26	6	$3.5e^{-5}$
	^{122}Sb	$1.2e^{-4}$	6.2	1.62	2.2	$1.3e^{-6}$
	^{110}Ag	$3e^{-4}$	89	0.88	0.3	$4.5e^{-7}$
^{239}Pu ($r_f = 0.35$)	^{128}I	$5.2e^{-3}$	6.2	1.26	6	$1.1e^{-4}$
	^{104}Rh	$6.8e^{-2}$	146	1.15	0.4	$9.4e^{-5}$
	^{110}Ag	$1.1e^{-2}$	89	0.88	0.3	$1.2e^{-5}$
	^{122}Sb	$4.3e^{-4}$	6.2	1.62	2.2	$3.5e^{-6}$

TABLE II: The core material compositions inside the reactor core containment vessel used in the neutron capture studies.

Functions	Materials	Weight (kg)
Fuel Elements	^{235}U	1376
	^{238}U	98688
	^{239}Pu	431
	^{241}Pu	84
Cooling	Water	42519
Control Rod Assembly at Complete Insertion	B_4C	479
	Zr-Alloy	67466
	Stainless Steel	14145
Support Structure	Stainless Steel	910000
Total Weight		157721

of the Kuo-Sheng(KS) Nuclear Power Station in Taiwan, where a neutrino laboratory[9] has been built. Standard “Watt” fission neutron spectrum parametrization[7, 8] were adopted as input: $\phi_n \propto \exp(-E/a) \sinh(\sqrt{bE})$ where (a,b) depend on the fission elements. There are on average 2.5 neutrons generated per fission. The neutrons are scattered in the core and eventually absorbed by either the (n,fission) processes with the fuel elements or the (n, γ) interactions with the core materials.

An important constraint is that an equilibrium chain reaction must be sustained to provide stable power generation. This is achieved by regulating the fraction of the control rod assembly(ξ) inserted into the fuel bundles. This constraint is parametrized by K_{eff} defined as the ratio of neutron-induced fissions to the starting fission rates. The variation of K_{eff} versus ξ is depicted in Figure 1. The equilibrium conditions require $K_{\text{eff}}=1$, and the distributions of the per-fission neutron capture

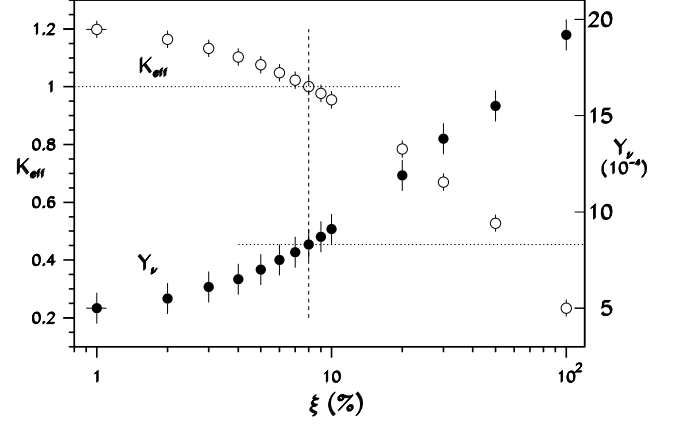


FIG. 1: The variation of the K_{eff} parameter and the neutrino yield Y_ν from ^{51}Cr as function of control rod fraction ξ .

TABLE III: The neutron capture yield Y_n (where $\Sigma Y_n=2.5$) of the major and relevant channels at $K_{\text{eff}}=1$.

Channel	Isotope	Weight (kg)	Y_n
(n,fission) on fuel element	^{238}U	98688	0.057
	^{235}U	1376	0.62
	^{239}Pu	431	0.26
	^{241}Pu	84	0.068
$\Sigma Y_n(\text{fission}) =$			1.0
(n, γ) at Core Region	^{238}U	98688	0.59
	Water	42500	0.25
	^{10}B	5.4	0.28
	^{50}Cr	9.0	0.00067
	^{54}Fe	26.6	0.00018
	^{58}Ni	57.6	0.0010
	^{50}Cr	8650	0.00016
Stainless Steel	^{54}Fe	38200	0.00012
	^{58}Ni	57300	0.00026
Containment Vessel			0.009
External to Containment Vessel			0.009

yield(Y_n) are given in Table III. Only 0.35% of the neutrons escape from the containment vessel, justifying that detailed treatment exterior to the vessel is not necessary.

Stainless steel and “Zr-2 alloy” are the typical construction materials at reactor cores, used in the containment vessel and control rod assembly, as well as in fuel-element containers, respectively. These materials contain chromium, iron and nickel which, upon activation by the (n, γ) reactions, produce ^{51}Cr , ^{55}Fe and ^{59}Ni that will subsequently decay by EC and ν_e emissions. Their properties (isotopic abundance IA, (n, γ) cross-sections $\sigma_{n\gamma}$, half-life $\tau_{1/2}$, EC Q-value and branching ratio BR) and ν_e -yield ($Y_\nu=Y_n \cdot \text{BR}$) are given in Table IV. The variation of Y_ν in ^{51}Cr with ξ is displayed in Figure 1. The half-life of ^{59}Ni is too long and thus not relevant for ν_e -emissions. The dominant reactor ν_e sources are therefore ^{51}Cr and ^{55}Fe , with total Y_ν of 8.3×10^{-4} and 3.0×10^{-4} ν_e /fission, implying total ν_e -fluxes of $7.5 \times 10^{16} \text{ s}^{-1}$ and $2.7 \times 10^{16} \text{ s}^{-1}$, respectively, at a 2.9 GW reactor. The

TABLE IV: The ν_e -sources and their yields Y_n , Y_ν (both in 10^{-4}) at the reactor core.

Isotope	IA(%)	$\sigma_{n\gamma}$ (b)	$\tau_{\frac{1}{2}}$	Q_{gs} (keV)	BR(%)	Y_n	Y_ν
^{103}Rh	4.6 [†]	146	41.8 s	1145	0.45	120 [‡]	0.54 [‡]
^{50}Cr	4.35	15.8	27.7 d	753	100	8.3	8.3
^{54}Fe	5.85	2.3	2.73 y	231	100	3.0	3.0
^{58}Ni	68.1	4.6	7.6e ⁴ y	1073	100	13.0	—

[†] fission yield

[‡] average over 18 months of irradiation

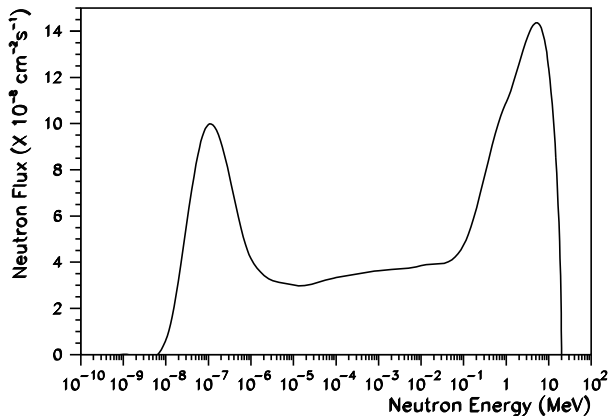


FIG. 2: Energy spectrum of neutron at the reactor core, derived from MCNP simulations.

total strength corresponds to a 2.7 MCi source. The integrated reactor $\nu_e/\bar{\nu}_e$ flux ratio at equilibrium is therefore $\sim 2 \times 10^{-4}$. In particular, the ν_e -e to $\bar{\nu}_e$ -e event rate ratio at the electron recoil energy range of 300 to 750 keV is expected to be 2×10^{-4} , too small to account for the factor of two excess over the Standard Model values in the measured $\bar{\nu}_e$ -e rates recently reported by the MUNU experiment[11].

To demonstrate the validity of the simulation procedures and results, a series of comparisons were made with industry-standard calculations and actual reactor operation data: (a) $\xi=8\%$ at $K_{\text{eff}}=1$ as shown in Figure 1, (b) the relative fission ratio of the four fissile elements, (c) the simulated neutron spectra at the reactor core, as depicted in Figure 2, which have a total flux of $1.8 \times 10^{14} \text{ cm}^{-2}\text{s}^{-1}$, with 28% in the thermal range, and (d) $Y_n=0.59$ for $^{238}\text{U}(n,\gamma)^{239}\text{U}$. Consistencies were achieved to within 10% in all cases. In particular, the important $^{238}\text{U}(n,\gamma)$ process leads to the accumulation of ^{239}Pu via β -decays of ^{239}U , and was independently studied[10]. These consistency requirements place constraints to possible systematic effects. The leading uncertainties arise from the modeling of the reactor core compositions, and were estimated to be $<20\%$.

A high-purity germanium detector has collected data with a trigger threshold of 5 keV at a distance of 28 m from the core at KS Plant. Background at the range of

$1/(\text{kg}\cdot\text{keV}\cdot\text{day})$ was achieved[12], comparable to those for underground Dark Matter experiments. This unique low energy data provides an opportunity to study directly the possible anomalous effects from reactor ν_e . While the sensitivities are not competitive to those from reactor $\bar{\nu}_e$, the studies provide direct probes on the ν_e properties without assuming CPT invariance, and cover possible anomalous matter effects which may differentiate ν_e from $\bar{\nu}_e$. The 18-month reactor cycle suggests that the optimal ν_e 's are from ^{51}Cr , where $\tau_{\frac{1}{2}}=27.7$ days. With the actual reactor OFF period denoted by $t=0$ to $t=67$ days, the background-measuring *OFF** period was taken to be from $t=30$ to 101 days, during which the average residual ν_e -flux was 37% of the steady-state ON-level.

The anomalous coupling of neutrinos with the photons are consequences of finite neutrino masses and electromagnetic form factors[13]. The manifestations include neutrino magnetic moments (μ_ν) and radiative decays (Γ_ν). The searches of μ_ν are performed in neutrino-electron scattering experiments, and the signature is an excess of events between reactor ON/OFF periods with an $1/T$ distribution, T being the energy of the recoil electron. Using 3458/1445 hours of ON/*OFF** data from KS, and adopting similar event selection and analysis procedures as Ref. [12], no excess of events was observed and a limit of $\mu_\nu(\nu_e) < 1.3 \times 10^{-8} \mu_B$ at 90% confidence level(CL) was derived. An indirect bound $\tau_\nu/m_\nu^3 > 5.7 \times 10^{14} \text{ eV}^3\text{s}$ at 90% CL for $\Gamma_\nu(\nu_e): \nu_e \rightarrow \nu_X + \gamma$ in vacuum can be inferred[13]. It is also of interest to perform a direct search on $\Gamma_\nu(\nu_e)$, the signature of which is a step-function modified by detector efficiencies at the ν_e energy[14]. No excess of events were observed between the ON/*OFF** data and a 90% CL limit of $\tau_\nu/m_\nu > 0.04 \text{ s eV}^{-1}$ for ν_e was derived. The direct $\Gamma_\nu(\nu_e)$ limit covers possible anomalous neutrino radiative decay mechanisms in matter. In particular, the matter-induced radiative decay rates can be enhanced by a huge factor($\sim 10^{23}$)[15] in the minimally-extended model. The residual plots for both searches are displayed in Figure 3. These results are complementary to the more stringent limits on ν_e from the previous accelerator experiments[16], by having lower neutrino energy and denser target density which may favor matter effects.

The merits of inserting selected materials to the reactor core to enhance the ν_e flux were investigated. A convenient procedure is to load them to the unfilled rods or to replace part of the UO_2 fuel elements during reactor outage. Though such a scenario involves difficulties with reactor operation regulations and requires further radiation safety studies, it is nevertheless technically feasible and ready — and costs much less than the accelerator-based neutrino factories projects[2]. It is therefore of interest to explore the physics potentials and achievable sensitivities. The candidate isotopes are those with good IA, $\sigma_{n\gamma}$ and BR as well as convenient lifetimes for the activated nuclei. To sustain chain reactions, the load should be less

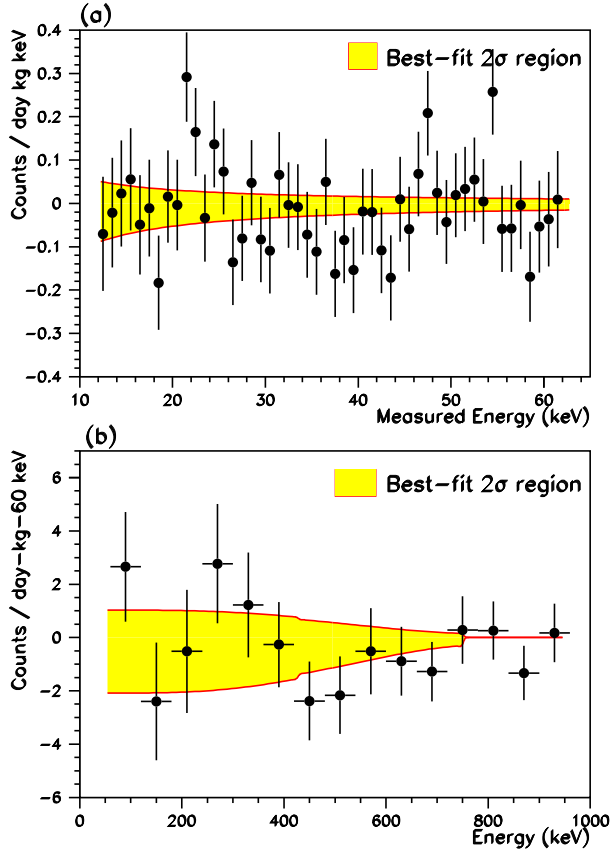


FIG. 3: Residual plots for neutrino (a) magnetic moment and (b) radiative decay searches with the reactor ^{51}Cr ν_e -source.

TABLE V: The maximal (n, γ) and ν_e yields for selected materials loaded to the reactor core.

Isotope	IA (%)	$\sigma_{n\gamma}$ (b)	$\tau_{1/2}$	Q (MeV)	BR (%)	Δ (%)	Y_n	Y_ν
$^{50}\text{Cr}(n)$	4.35	15.8	27.7 d	753	100	14.3	0.056	0.056
$^{50}\text{Cr}(p)$	100					4.8	0.28	0.28
$^{63}\text{Cu}(n)$	69.2	4.5	12.7 h	1675	61	16.3	0.20	0.12
$^{63}\text{Cu}(p)$	100					14.8	0.25	0.15
$^{151}\text{Eu}(n)$	47.8	2800	9.3 h	1920	27	0.073	0.092	0.025
$^{151}\text{Eu}(p)$	100					0.035	0.095	0.027

than certain critical value to keep $K_{\text{eff}}=1$ viable. Several selected materials and their maximum Y_n and Y_ν at $K_{\text{eff}}=1$ in both natural(n) and pure(p) IA form are given in Table V. The amount of necessary inserted materials as a fraction of the fuel-element mass are denoted by Δ . The optimal choice is $^{50}\text{Cr}(p)$ where $Y_\nu=0.28$. This is equivalent to a 1 GCi source for a 4.5 GW reactor, where the ν_e flux at 10 m is $3 \times 10^{12} \text{ cm}^{-2}\text{s}^{-1}$.

In order to detect such neutrinos, detection mechanisms common to both ν_e and $\bar{\nu}_e$ such as neutrino-electron scatterings are not appropriate. Instead, flavor-specific charged-current interactions ($\nu_e\text{NCC}$) would be ideal. Solar ν_e has been observed by $\nu_e\text{NCC}$ in radio-

TABLE VI: Expected $\nu_e\text{NCC}$ rates per ton-year at a reactor ^{51}Cr ν_e -flux of $3 \times 10^{12} \text{ cm}^{-2}\text{s}^{-1}$ (R_{core}), at the standard solar model ^7Be flux (R_\odot), and due to a 1 MCi ^{51}Cr source (R_{src}).

Target	IA(%)	Threshold(keV)	R_{core}	R_\odot	R_{src}^\dagger
^{71}Ga	39.9	236	1900	3.8	58
^{100}Mo	9.63	168	2100	3.9	64
^{115}In	95.7	118	9900	19	300
^{176}Yb	12.7	301	3400	7.4	100

† for four half-lives of data taking.

chemical experiments on ^{37}Cl and ^{71}Ga , with calibration measurements using ^{51}Cr ν_e -sources performed for ^{71}Ga [1, 2]. Detection of the low energy solar neutrinos has been a central topic in neutrino physics. There are many schemes and intense efforts toward counter experiments with $\nu_e\text{NCC}$ [17], using isotopes such as ^{100}Mo , ^{115}In , ^{176}Yb . The $\nu_e\text{NCC}$ rates for the various isotopes in their natural abundance at a ^{51}Cr ν_e -flux of $3 \times 10^{12} \text{ cm}^{-2}\text{s}^{-1}$ are summarized in Table VI. Also listed for comparison are the rates from the standard solar model ^7Be ν_e -flux and from a 1 MCi ^{51}Cr source inside a spherical detector of 1 m diameter. About 10^4 $\nu_e\text{NCC}$ events or 1% statistical accuracy can be achieved by one ton-year of data with an ^{115}In target. Calculations of the ν_e flux depends on the amount of loaded materials and the well-modeled reactor neutron spectra, so that a few % accuracy should be possible. Similar uncertainties can be expected on the $\nu_e\text{NCC}$ cross-section measurements. This would provide important calibration data to complement the solar neutrino program.

Such mono-energetic ν_e neutrino sources can be used to study the mixing angle θ_{13} . They allow better systematic control than with fission $\bar{\nu}_e$'s[18]. The rates from simple counting experiments between *NEAR* and *FAR* detectors can be compared to look for possible deviations from $1/L^2$, L being the core-detector distance. The ν_e -flux can be accurately measured by the *NEAR* detectors. Considering both oscillation and luminosity effects, the sensitivities at a given neutrino energy E_ν depend on $[\sin^2(\frac{\Delta m^2 L}{E_\nu})]/\sqrt{L^2}$. The optimal distance for the *FAR* detector with $\Delta m^2=0.002 \text{ eV}^2$ and $E_\nu=747 \text{ keV}$ from the ^{51}Cr -source is therefore $L_0 \sim 340 \text{ m}$. Table VII shows the achievable sensitivities to $\sin^2 2\theta_{13}$ with various detector options in both natural(n) and pure(p) IA located at L_0 from a two-core power plant each with $P_{\text{th}}=4.5 \text{ GW}$. The source strength of $Y_\nu=0.28 \nu_e/\text{fission}$ for maximally-loaded ^{51}Cr in Table V is adopted. A $<1\%$ sensitivity level can be achieved with 5 years of data taking using a 100 ton target – comparable to the other reactor- and accelerator-based projects.

Another possibility is on the monitoring of unwaranted plutonium production during reactor operation – an issue of paramount importance in the control of nuclear proliferation[19]. Plutonium is primarily produced

TABLE VII: Sensitivities to θ_{13} from maximally-loaded reactor core with $^{51}\text{Cr}(\text{p})$ sources for different detector options. Listed are event rates per 500-ton-year (R_{500}), their achievable 1σ statistical (σ_{500}) and $\sin^2 2\theta_{13}(\delta(\sin^2 2\theta_{13}))$ accuracies.

Target	IA(%)	R_{500}	$\sigma_{500}(\%)$	$\delta(\sin^2 2\theta_{13})$
$^{100}\text{Mo}(\text{n})$	9.6	1800	2.4	0.029
$^{100}\text{Mo}(\text{p})$	100	18000	0.74	0.009
$^{115}\text{In}(\text{n})$	95.7	8200	1.1	0.013
$^{176}\text{Yb}(\text{n})$	12.7	2800	1.9	0.021
$^{176}\text{Yb}(\text{p})$	100	22000	0.67	0.0077

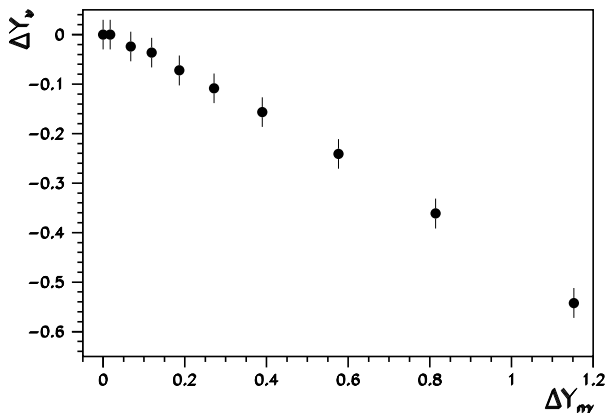


FIG. 4: Simulated correlations between the fractional changes of ν_e -yield (ΔY_{ν_e}) from a reactor ^{51}Cr ν_e -source versus those for the $^{238}\text{U}(\text{n}, \gamma)^{239}\text{U}$ reaction ($\Delta Y_{\text{n}\gamma}$). The error bars assume a 3% measurement error of Y_{ν_e} .

by β -decays following $^{238}\text{U}(\text{n}, \gamma)^{239}\text{U}$ whose cross-section is overwhelmed at high energy (>1 eV)[6]. In contrast, the $\sigma(\text{n}, \gamma)$ in Table V which give rise to ν_e -emissions are pre-dominantly thermal. The control rod and the cooling water fractions can be optimized to modify the core neutron spectra without changing the fission rate. Measurements of the ν_e NCC rates is an effective means to probe the neutron spectra, and therefore to monitor directly the ^{239}Pu accumulation, as depicted in Figure 4 in the case for ν_e from ^{51}Cr . A 10% enhancement of the ^{239}Pu production rate leads to a 4% reduction of the ν_e flux. Using results from Table VI as illustrations, such changes can be detected at the 3σ level at a 4.5 GW

power reactor with a maximally-loaded ^{51}Cr source by a 10-ton indium detector at 10 m in 21 days.

The authors are grateful to Drs. Z.L. Luo and Y.Q. Shi for discussions on reactor neutron simulations. This work was supported by grants 91-2112-M-001-036/92-2112-M-001-057 from the National Science Council, Taiwan, and 19975050 from the National Science Foundation, China.

* Corresponding Author: ht Wong@phys.sinica.edu.tw

- [1] See the respective sections in *Review of Particle Physics*, Phys. Lett. **B 592**, 1 (2004), for details and references.
- [2] *Proc. of the XXI Int. Conf. on Neutrino Phys. & Astrophys., Paris*, ed. J. Dumarchez, Nucl. Phys. **B** (Proc. Suppl.), in press (2005).
- [3] H.B. Li and H.T. Wong, J. Phys. **G 28**, 1453 (2002), and references therein.
- [4] B. Achkar et al., Phys. Lett. **B 374**, 243 (1996).
- [5] S.M. Blankenship, Internal Report, UC Irvine, unpublished (1976); K. Schreckenbach, Internal Report, ILL Grenoble, unpublished (1984).
- [6] Evaluation and Compilation of Fission Yields, T.R. England and B.F. Rider, ENDF-349, LA-UR-94-3106 (1993).
- [7] A General Monte Carlo N-particle Transport Code, Version 4A, J. F. Briesmeister ed., LA-12625-M (1997).
- [8] W.M. Stacey, Nuclear Reactor Physics, Wiley (2001).
- [9] H.T. Wong, Mod. Phys. Lett. **A 19**, 1207 (2004), and references therein.
- [10] V.I. Kopeikin, L.A. Mikaelyan, and V.V. Sinev, Phys. Atomic Nuclei **60**, 172 (1997).
- [11] Z. Daraktchieva et al., Phys. Lett. **B 564**, 190 (2003).
- [12] H.B. Li et al., Phys. Rev. Lett. **90**, 131802 (2003).
- [13] H.T. Wong, hep-ex/0409003 (2004), also in Ref. [2], and references therein.
- [14] F. Vannucci, in *Proc. of Neutrino Telescope Workshop, 1999*, ed. M. Baldo-Ceolin, Vol. **1**, 165 (1999).
- [15] C. Giunti, C.W. Kim, and W.P. Lam, Phys. Rev. **D 43**, 164 (1991).
- [16] D.A. Krakauer et al., Phys. Rev. **D 44**, R6 (1991); R.C. Allen et al., Phys. Rev. **D 47**, 11 (1993); L.B. Auerbach et al., Phys. Rev. **D 63**, 112001 (2001).
- [17] R.S. Raghavan, Phys. Rev. Lett. **37**, 259 (1976); R.S. Raghavan, Phys. Rev. Lett. **78**, 3618 (1997); H. Ejiri et al., Phys. Rev. Lett. **85**, 2917 (2000).
- [18] K. Anderson et al., hep-ex/0402041 (2004).
- [19] J. Learned, in Ref. [2], and references therein.